Theoretical analysis of the emission spectra of the NaCd excimer

C. Angeli, M. Persico, M. Allegrini, G. De Filippo, F. Fuso, D. Gruber, L. Windholz, and M. Musso

Citation: The Journal of Chemical Physics **102**, 7782 (1995); doi: 10.1063/1.469031
View online: http://dx.doi.org/10.1063/1.469031
View Table of Contents: http://scitation.aip.org/content/aip/journal/jcp/102/20?ver=pdfcov
Published by the AIP Publishing

Theoretical analysis of the emission spectra of the NaCd excimer

C. Angeli and M. Persico
Dipartimento di Chimica e Chim. Ind., Università di Pisa, v. Risorgimento 35, I-56126 Pisa, Italy

M. Allegrini,[a] G. De Filippo, and F. Fuso
Dipartimento di Fisica, Università di Pisa, p.za Torricelli 2, I-56125 Pisa, Italy

D. Gruber and L. Windholz
Institut für Experimentalphysik, Technische Universität Graz, Petersgasse 16, A-8010 Graz, Austria

M. Musso
Institut für Physik und Biophysik, Universität Salzburg, Hellbrunnerstrasse 34, A-5020 Salzburg, Austria

(Received 30 December 1994; accepted 8 February 1995)

We present simulations of bound–bound and bound–free emissions of the NaCd* excimer, along with new experimental results concerning the red band system. The simulations, based on *ab initio* potential energy curves, confirm that the initial states are $2\ ^2\Sigma^+$ for the red emission and $2\ ^2\Pi$ for the blue emission of NaCd*. The two main peaks in the blue band system are due to spin–orbit splitting. The band shape obtained in the simulations is extremely variable, depending on the population distribution of the vibrational states of NaCd*. The comparison of simulated and measured spectra leads us to conclude that, in the experimental conditions adopted here and in previous work, the thermal equilibration of the excimer is far from complete. © *1995 American Institute of Physics.*

I. INTRODUCTION

Emission spectra of intermetallic excimers of elements of the I A and II B groups have been studied by means of a variety of experimental techniques. The excimers have been produced in high pressure lamps, molecular beams, and heat-pipe ovens. Two emission band systems have been generally observed. The ''red'' bands are in the 600–900 nm range for NaCd,[1–3] NaHg,[4–6] or KHg.[7] ''Blue'' or ''blue–green'' bands are found at 450–500 nm for LiZn,[8,9] LiCd,[9,10] LiHg,[11] NaZn,[12] NaCd,[3,13–16] or NaHg;[13,14] for KCd[17] and KHg[7] the emission is placed at longer wavelengths, $\simeq$620 nm. We have limited this overview to the first three alkali metals. A comprehensive discussion of intermetallic excimer emissions has been given by Milošević.[18]

Among the nine possible combinations of Li, Na, and K, with Zn, Cd, and Hg, here envisaged, NaCd is the most thoroughly studied from the experimental point of view. NaCd* (here the suffix $*$ indicates electronic excitation) has been produced in discharge lamps[1] and in heat-pipe ovens;[2,3,13–16] experiments in cells are in progress in our laboratory in Pisa. At least two photochemical reactions have been shown to generate NaCd*. Following the laser excitation of Na_2 with wavelengths ranging from 308 to 515 nm, we have

$$Na_2^* + Cd \rightarrow NaCd^* + Na. \tag{1}$$

When exciting the Cd atoms to the $5p\ ^3P_1$ metastable state, an important process is

$$Cd^* + Na_2 \rightarrow NaCd^* + Na \tag{2}$$

although at sufficiently high total pressures a three-body collision may also take place:

$$Cd^* + Na + M \rightarrow NaCd^* + M. \tag{3}$$

Both the red and the blue band systems of NaCd* have been observed, and the decay of the blue emission following pulsed laser excitation has been monitored.[3,14,16]

On the other hand, a theoretical analysis of the emission bands of NaCd has not yet been presented. For most of the other excimers the lowest potential energy curves have been computed by means of rather accurate CI methods. All electron nonrelativistic calculations have been performed for LiZn,[8] LiCd,[10] and NaZn;[12] relativistic theory, including spin–orbit coupling, has been applied to LiHg[11] and NaHg;[13] semiempirical pseudopotentials, incorporating relativistic effects, have been employed in the case of KHg.[19] The computed transition energies and the dipole moments have led us to identify the emitting states as the second (first excited) $^2\Sigma^+$ and the second $^2\Pi$ for the red and blue bands, respectively. These assignments are substantially valid for all excimers, although in the Hg compounds the spin–orbit coupling induces a strong mixing of the $2^2\Pi$ state with the close lying $3^2\Sigma^+$.

Partial simulations of the emission bands have been published for LiZn[8] and NaZn:[12] only bound–free transitions at a fixed angular momentum J were considered. Only very recently have Li *et al.*[9] performed more complete simulations, showing the importance of bound–bound transitions in the cases of LiZn and LiCd (see also Milošević[18]). The free–free and bound–free emissions of Na+Hg in high-pressure discharge lamp have also been analyzed.[4,5]

In Sec. II we present a new observation of the emission spectrum of NaCd* (red bands), produced in a heat-pipe oven by the photochemical reaction (1). Sections III and IV report the analysis of the red and blue bands, based on a

[a]Present address: Dipartimento di Fisica della Materia, Geofisica, Fisica dell'Ambiente, Università di Messina, Salita Sperone 31, 98166 Sant'Agata-Messina, Italy

 0021-9606/95/102(20)/7782/7/$6.00

complete simulation of the emission spectrum: bound–free and bound–bound transitions starting from all vibrational and rotational states are considered. The radiative lifetimes of the emitting states are evaluated and attention is paid to the question whether or not the population of the vibrational states of the excimer is thermalized. The spectral simulations are based on potential energy curves and transition dipoles, computed with *ab initio* methods including the main relativistic effects in effective core potentials.[20,21]

II. EXPERIMENT

The fluorescence spectra collected in the blue region during excitation of the Na+Cd vapor mixture, as well as the investigation of the time behavior of the fluorescence signal, have already been presented elsewhere.[3,14,16] They demonstrate the presence of four different bands, located around 484.3, 479.1, 473.5, and 467 nm, here labeled $B_1,...,B_4$, respectively. Briefly, the vapor mixture, contained in a heat-pipe oven filled with argon as buffer gas at pressure p in the range 35–80 mbar and maintained at a temperature T in the range 520–850 K, has been irradiated with a laser beam. Both pulsed and cw laser sources have been used. Pulsed excitation was provided by either an excimer laser ($\lambda=308$ nm) or a dye laser pumped by the same excimer laser and tunable on a wavelength range allowing the resonant excitation of the Cd $5p\ ^3P_1$ level; in cw experiments, a single line Ar^+ laser ($\lambda=488$ nm) has been used.

The fluorescence emission of the vapor mixture has been collected at right angle with respect to the direction of the excitation beam and analyzed by means of a monochromator (64 cm focal length) equipped with a fast photomultiplier. In cw experiments, lock-in detection has been utilized. In the case of pulsed excitation, the fluorescence signal has been either time integrated by a boxcar averager or directly recorded by a digital oscilloscope for acquisition of spectra or analysis of the time behavior of the fluorescence, respectively.

A spectrum of the red region, following cw excitation of the Na+Cd mixture, at $T=850$ K and $p=80$ mbar, is shown here as an example (see Fig. 5). The NaCd* emission in this range is characterized by the presence of five bands, located around 723.9, 714.8, 707.9 (a shoulder of the preceding one), 696.2, and 688 nm, here labeled $R_1,...,R_5$, respectively.

The effective lifetime of NaCd* in the blue region has been determined as a function of the excitation wavelength, which allows one to exploit different reaction channels. The observed decay time for the fluorescence emission is strongly influenced by the lifetime of the colliding partners. For the excimer formation involving the Na_2 excitation (channel 1), an effective lifetime in the tens of nanoseconds range has been observed.[14] For resonant excitation of the Cd atom (channels 2,3), the effective lifetime lies in the microsecond range, as expected due to the long lifetime of the $5p\ ^3P_1$ Cd level.[17] These observations suggest that the spontaneous lifetime of NaCd* itself, in the given experimental conditions, is of the order of 10 ns, or even shorter.

III. SIMULATION OF EMISSION SPECTRA

A detailed description of the *ab initio* calculations is given elsewhere:[20,21] here we simply summarize it for a better comprehension of the simulations. The NaCd molecular orbitals were determined by a restricted HF calculation, followed by a unitary transformation to obtain localization on the two atoms and concentration of the lowest energy diffuse virtuals. The inner shells of Cd were replaced by relativistic *ab initio* effective core potentials.[22] A contracted Gaussian basis set $[12s9p7d]$ was employed for Na, and $[4s4p4d2f]$ for Cd.

The electron correlation was treated by means of quasidegenerate perturbation theory (QDPT) in the CIPSI version.[23,24] Quasidiabatic (QD) states have been determined by means of a technique put forward by one of us.[25,26] The QD states can be approximately identified with products of atomic states: Na($3\ ^2S$, $3\ ^2P$, $4\ ^2S$, $3\ ^2D$,$4\ ^2P$, $5\ ^2S$) Cd($5\ ^1S$) and Na($3\ ^2S$) Cd($5\ ^3P$). The nature of the QD states is substantially independent on the internuclear distance R, therefore it is justified to apply constant shifts to the computed diabatic energies, in order to bring their asymptotic values in perfect agreement with the known atomic transition energies.[27] Spline interpolation and diagonalization of the QDPT Hamiltonian matrix $\mathbf{H}_{\mathrm{QDPT}}$, computed at several values of R in the QD basis, yields the adiabatic states and energies, and the radial nonadiabatic couplings.

The effect of the spin–orbit coupling on the potential energy curves can be evaluated, again exploiting the approximate invariance of the QD wave functions on the R distance. We can assume that the spin–orbit Hamiltonian matrix in the QD basis, $\mathbf{H}_{\mathrm{SO}}$, does not depend on R. For the separate atoms ($R=\infty$) $\mathbf{H}_{\mathrm{SO}}$ is known. We add it to $\mathbf{H}_{\mathrm{QDPT}}(R)$ to obtain the complete Hamiltonian matrix:

$$\mathbf{H}(R)=\mathbf{H}_{\mathrm{QDPT}}(R)+\mathbf{H}_{\mathrm{SO}}. \tag{4}$$

The potential energy curves incorporating the spin–orbit interaction are the eigenvalues of $\mathbf{H}$. Figure 1 shows the curves corresponding to the lowest states: actually more electronic states have been computed, including those which dissociate to Cd $5\ ^3P$. All the possible candidates to the role of emitting states for the red and blue band systems are presented in the figure. As in other excimers, the lowest excited states, and particularly the $^2\Pi$ states, are more bound than the ground state. The $1\ ^2\Pi$ and $2\ ^2\Pi$ potentials are split, because of the spin–orbit interaction. However, in the following discussion we shall treat the $^2\Pi_{1/2}$ and $^2\Pi_{3/2}$ components as a single state, whenever it is not important to consider them separately.

We also determined the transition dipoles connecting the excited states and the ground state: they are shown in Fig. 2, as functions of R. For $R=\infty$ our computed dipoles reproduce the experimental oscillator strengths of Na with a good accuracy, as shown in Table I (largest relative error, 11%, for the $3s\rightarrow 3p$ transition). Figure 3 shows the difference potential (DP) curves between the lowest excited states and the ground state. According to Mulliken's semiclassical treatment,[28] a minimum in the difference potential corresponds to a sharp peak in the emission spectrum. The DP of the $2\ ^2\Sigma^+$ and $2\ ^2\Pi$ states exhibit well defined minima: the

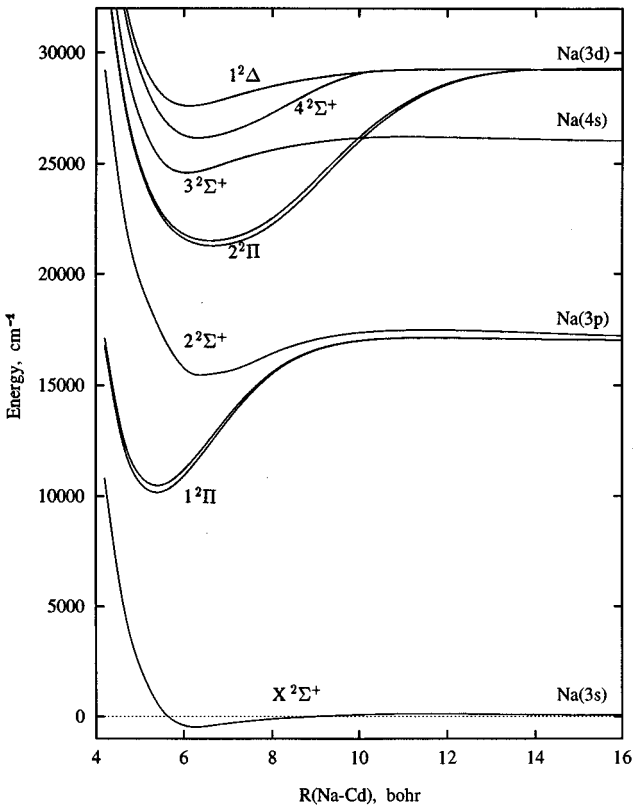

FIG. 1. Potential energy curves of NaCd, including spin–orbit coupling.

transition energies approximately agree with those of the red and blue emissions, respectively. The lowest excited state $1\ ^2\Pi$ has no extremum in the DP, and the shallow minimum in the $3\ ^2\Sigma^+$ DP is too high in energy. Moreover, the transition dipoles between the ground state and $2\ ^2\Sigma^+$ or $2\ ^2\Pi$ are larger, respectively, than those between ground state and $1\ ^2\Pi$ or $3\ ^2\Sigma^+$. On the basis of these considerations, the emitting state for the red band system is $2\ ^2\Sigma^+$ and for the blue system is $2\ ^2\Pi$. In the following we shall concentrate our attention on these states and try to reproduce the experimental spectra through theoretical simulations.

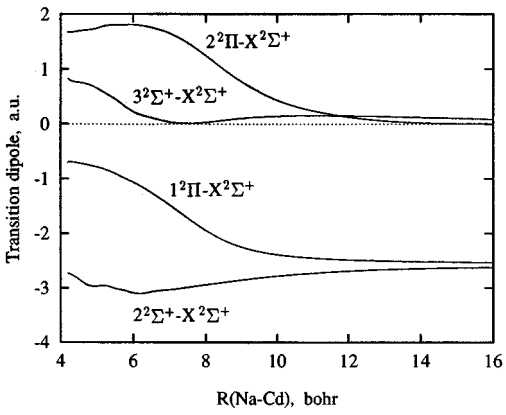

FIG. 2. Computed transition dipoles from the $2\ ^2\Sigma^+$, $3\ ^2\Sigma^+$, $1\ ^2\Pi$, and $2\ ^2\Pi$ states to the ground state.

TABLE I. Computed and experimental oscillator strengths for the Na atom.

Transition	$f_{\text{calc.}}$	$f_{\text{expt.}}$
$3s\rightarrow 3p$	1.0532	0.9468
$3s\rightarrow 4p$	0.0132	0.0154
$3p\rightarrow 4s$	0.1726	0.1644
$3p\rightarrow 5s$	0.0142	0.0135
$4s\rightarrow 4p$	1.5196	1.4320
$4p\rightarrow 5s$	0.3131	0.3106

The spectral simulations based on the electronic energies and transition dipoles involve the following steps: (1) determination of the vibrational states; (2) calculation of bound–free and bound–bound oscillator strengths; (3) sum over J (angular momentum quantum number) to obtain the contribution to the emission spectrum of a given initial vibrational state v'; (4) sum over v' according to the assumed distribution of the initial state populations.

The bound and dissociative vibrational states were determined by the Numerov method, in a version similar to Hajj's,[29] which allows us to change both the starting and end point of the numerical integration according to the features of each vibrational state. For a given J we computed all the bound levels in the upper ($2\ ^2\Sigma^+$ or $2\ ^2\Pi$) and lower ($X\ ^2\Sigma^+$) potential, respectively $|G_{UJv'}\rangle$ and $|G_{LJv''}\rangle$, with energies $\varepsilon_{UJv'}$ and $\varepsilon_{LJv''}$. Dissociative vibrational states $|G_{LJ\varepsilon}\rangle$ in the ground state potential were obtained for a set of equally spaced energies ε. The $|G_{LJ\varepsilon}\rangle$ were normalized so that $\langle G_{LJ\varepsilon}|G_{LJ\varepsilon'}\rangle=\delta(\varepsilon-\varepsilon')$. In the vibrational Schrödinger equation the contribution of the electronic spin to the total angular momentum was neglected (an error of the order of 1 cm^{-1} in the centrifugal potential): therefore we may

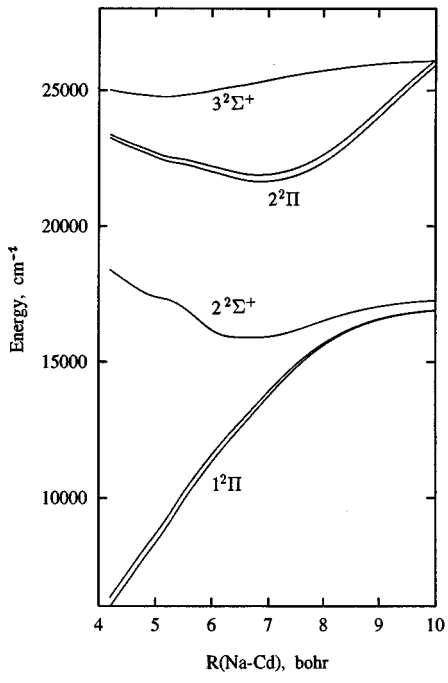

FIG. 3. Difference potentials between the $2\ ^2\Sigma^+$, $3\ ^2\Sigma^+$, $1\ ^2\Pi$, and $2\ ^2\Pi$ states and the ground state.

consider integer J. We actually ran calculations for J equal to an integer multiple of 5, $J=0,5,...,J_{\max}$. The contributions to the emission spectra from states with other J values were made up by interpolation (see below). $J_{\max}$ was 140 for the $2\ ^2\Sigma^+$ initial state, because for higher J no more bound vibrational states are found. $J_{\max}=150$ was set for the $2\ ^2\Pi$ state, because the Boltzmann factors for higher J are negligibly small.

The transition dipoles $\langle G_{UJv'}|\boldsymbol{\mu}|G_{LJv''}\rangle$ and $\langle G_{UJv'}|\boldsymbol{\mu}|G_{LJ\varepsilon}\rangle$ were computed by numerical quadrature. For the bound–free transitions we directly obtain the contribution to the oscillator strength or spectral density, as a function of the emitted frequency $\nu=(\varepsilon_{UJv'}-\varepsilon)/(2\pi)$:

$$\left(\frac{df}{d\nu}\right)_{Jv'}^{(b-f)}=\frac{4\pi}{3}(\varepsilon_{UJv'}-\varepsilon)|\langle G_{UJv'}|\boldsymbol{\mu}|G_{LJ\varepsilon}\rangle|^2 \tag{5}$$

(atomic units are used, $\hbar=1$). In order to sum up bound–free and bound–bound contributions in a consistent way, we assumed that the bound–bound resonances are broadened, with an arbitrary width $\Delta\nu$, set equal to half of the spacing between vibrational levels in the ground state ($\Delta\nu=50\ \ \mathrm{cm}^{-1}$). Therefore, while the oscillator strength of a single bound–bound transition is

$$f_{Jv'v''}=\tfrac{2}{3}(\varepsilon_{UJv'}-\varepsilon_{LJv''})|\langle G_{UJv'}|\boldsymbol{\mu}|G_{LJv''}\rangle|^2 \tag{6}$$

the contribution of all bound–bound transitions starting from the J,v' level, to the emission frequency ν, is

$$\left(\frac{df}{d\nu}\right)_{Jv'}^{(b-b)}=\sum_{v''}\frac{f_{Jv'v''}}{\sqrt{\pi}\Delta\nu}e^{-(\nu-\nu_{Jv'v''})^2/\Delta\nu^2}. \tag{7}$$

Here $\nu_{Jv'v''}=(\varepsilon_{UJv'}-\varepsilon_{LJv''})/(2\pi)$ is the resonance frequency. We only consider Q branch transitions, because the variation of the centrifugal potential for an increment ±1 in J is of the order of 1 cm^{-1}, leading to negligible differences in the wave functions and P or R branch frequencies and oscillator strengths.

The spectral density contribution for the emitting state J,v' is $(df/d\nu)_{Jv'}^{(b-f)}+(df/d\nu)_{Jv'}^{(b-b)}$, and the total emission is given by a sum over the initial states:

$$\left(\frac{df}{d\nu}\right)^{(\mathrm{tot})}=\sum_{v'}N_{v'}\sum_{J}N_{Jv'}\left[\left(\frac{df}{d\nu}\right)_{Jv'}^{(b-f)}+\left(\frac{df}{d\nu}\right)_{Jv'}^{(b-b)}\right]. \tag{8}$$

Here the product of the vibrational and rotational factors $N_{v'}N_{Jv'}$ is proportional to the population of the J,v' state. As we did not explicitly calculate all the terms in the second summation (index J), we treated it as an integral in the variable J and we evaluated it by the Simpson rule; a few tests showed that computing $(df/d\nu)_{Jv'}^{(b-f)}+(df/d\nu)_{Jv'}^{(b-b)}$ for J values with a spacing of five units is sufficient to get a good numerical accuracy.

IV. SIMULATION RESULTS AND DISCUSSION

We can only make some reasonable assumptions concerning the population of the J,v' excimer states. A validation of such assumptions at present can only come from the comparison of measured and simulated spectra. The main problem is that we do not know what is the initial distribution resulting from the reactive processes (1)–(3), nor to what extent such distribution is modified by further collisions of the excimer with Cd, Na, or Ar atoms (the concentration of Na_2 molecules is about 30 times smaller than that of Na, therefore Na_2 can be neglected as an effective collisional partner). A complete thermalization of the excimer state population is possible only if NaCd* undergoes several collisions during its lifetime τ. τ depends primarily on the emission rate τ_{rad}^{-1}, and possibly on a predissociation rate $\tau_{\mathrm{pred}}^{-1}$. Moreover, not all the collisions will simply change the J,v' state of NaCd*: they may also lead to dissociation of the excimer, thus shortening the lifetime.

We evaluated the predissociation rates of the $2\ ^2\Sigma^+$ state to $X\ ^2\Sigma^+$ and of $2\ ^2\Pi$ to $1\ ^2\Pi$. To this end we computed the radial nonadiabatic coupling between bound vibrational wave functions in the initial electronic state and dissociative wave functions in the final state; we then applied Fano's theory of discrete–continuum interactions[30] (the formulas and an example of application of the theory of diatomic predissociation by nonadiabatic coupling can be found in Ref. 31). The computed predissociation rates were very low for all states: $\tau_{\mathrm{pred}}>10^5$ ns. Therefore we can disregard this decay channel in the following discussion.

The radiative decay rate of a J,v' state is related to the oscillator strengths by

$$\tau_{\mathrm{rad}}^{-1}=\frac{2}{c^3}\sum_{v''}(\varepsilon_{UJv'}-\varepsilon_{LJv''})^2 f_{Jv'v''}+\frac{2}{c^3}\int_0^\infty 4\pi^2\nu^2\left(\frac{df}{d\nu}\right)_{Jv'}^{(b-f)}d\nu. \tag{9}$$

In Table II we show the radiative lifetimes for several J,v' states belonging to $2\ ^2\Sigma^+$ and to $2\ ^2\Pi$, and the relative contribution of the bound–bound transitions to the rate τ_{rad}^{-1} [first term in Eq. (9), i.e., the sum over v'']. The bound–bound contribution to the decay rates is also a measure of the overall importance of these transitions in the emission spectrum. The relative weight of bound–bound and bound–free transitions is extremely dependent on the initial quantum numbers v' and J, but the total lifetime is much less affected. The most populated rotational states according to a Boltzmann distribution, those with $J\simeq60$, show a moderate prevalence of the bound–free transitions in the average. The lifetimes τ_{rad} are of the order of 20 ns for $2\ ^2\Sigma^+$ and 30 ns for $2\ ^2\Pi$. Taking into account that the collisions can possibly shorten the total lifetime, these values are consistent with the experimental measurements (see end of Sec. II).

The estimate of the mean time between two collisions of molecule A with partner B, is based on the equation

$$\tau_{\mathrm{coll}}^{-1}=\left(\frac{2}{\pi m_{\mathrm{AB}}kT}\right)^{1/2}\sigma_{\mathrm{AB}}p_{\mathrm{B}}. \tag{10}$$

Here m_{AB} is the reduced mass, σ_{AB} is the cross section, and p_{B} is the partial pressure of B. We do not know the partial pressures of Na, Cd, and Ar, although probably Cd is the most abundant of the three, because of the conditions existing in the heat-pipe and because its vapor pressure is higher

TABLE II. Radiative lifetimes (ns) and bound–bound contributions to the transition rates, for several J,v' emitting states in the $2\ ^2\Sigma^+$ and $2\ ^2\Pi$ potentials.

		$2\ ^2\Sigma^+$		$2\ ^2\Pi$	
J	v'	τ_{rad}	bound–bound	τ_{rad}	bound–bound
0	0	79	100%	16	100%
0	2	68	100%	17	100%
0	4	25	34%	19	100%
0	8	19	28%	19	43%
0	12	18	14%	20	7%
30	0	13	100%	17	100%
30	2	13	100%	17	100%
30	4	13	65%	22	92%
30	8	16	30%	24	26%
30	12	16	23%	20	7%
60	0	13	100%	17	100%
60	2	16	100%	35	97%
60	4	29	35%	36	60%
60	8	20	1%	26	1%
60	12	17	0%	21	0%
90	0	5200	0%	1600	0%
90	2	200	0%	52	0%
90	4	17	0%	25	0%
90	8	15	0%	20	0%
120	0	13	0%	18	0%
120	2	13	0%	18	0%
120	4	13	0%	18	0%

than that of Na. The total pressure is equal or slightly larger than the initial buffer gas pressure, i.e., 80 mbar during the red bands measurements, and 35 mbar for the blue bands. The cross sections for collisions of NaCd with Na, Cd, and Ar, as deduced from the atomic radii, are all close to about 140 Å^2. With these parameters we obtain $\tau_{coll}=4-7$ ns for the $2\ ^2\Sigma^+$ state (red bands) and $\tau_{coll}=9-17$ ns for the $2\ ^2\Pi$ state (blue bands): the lower limits correspond to the lightest colliding partner (Na), the higher ones to Cd. Comparing these estimates with the lifetimes τ_{rad}, we conclude that each excimer molecule undergoes in the average only a few collisions before emitting. Therefore, only a partial thermalization of the excited state populations is probably achieved.

We shall assume that the rotational states with a given v' are populated according to the Boltzmann distribution, because the rotational thermalization is usually faster than the vibrational one:

$$N_{Jv'}=(2J+1)e^{-(\varepsilon_{UJv'}-\varepsilon_{U0v'})/kT}. \tag{11}$$

Here the difference $\varepsilon_{UJv'}-\varepsilon_{U0v'}$ plays the role of the rotational energy, as the rovibrational levels are determined exactly, without resorting to an approximate decoupling of vibration and rotation. We can now determine the contribution to the emission of a single vibrational state, by performing the second summation (index J) in Eq. (8).

Figure 4 shows the computed emission spectra, in the hypothesis that the initial state is $2\ ^2\Sigma^+$ with given v'. The band structure changes widely with v'. The lowest v' produce sharp peaks, mainly due to bound–free transitions with high J, all summing-up to the same wavelength. Higher vibrational states give several maxima, approximately as many

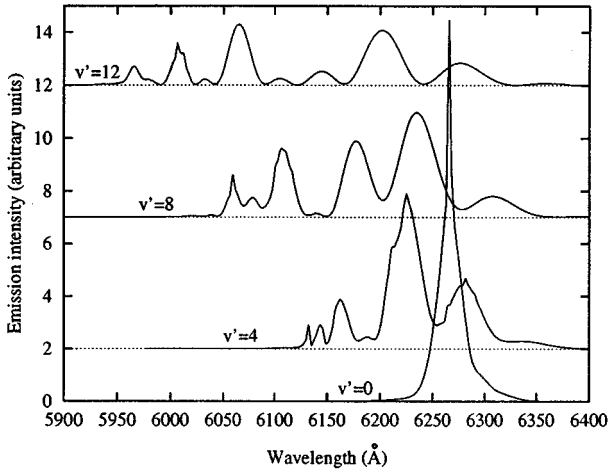

FIG. 4. Emission from the $2\ ^2\Sigma^+$ state; simulated spectra, in the hypothesis that a single vibrational level v' is populated.

as the quantum number v', due to the variation of the transition dipole integrals. The latter are large whenever the initial, bound, wave function, and the final one (bound or dissociative), are approximately in phase for several oscillations: this condition can be met for different transition energies, according to the position of the first maximum in the final wave function (close to the turning point of the repulsive limb of the lower potential).

Obviously none of the partial spectra with fixed v' reproduces the experimental spectrum, shown in Fig. 5, although, for intermediate v', the spacing between contiguous maxima is approximately correct. In summing up the contributions of all states, we have tested some different assumptions about the vibrational state distribution. According to Boltzmann's law, we should have

$$N_{v'}=e^{-\varepsilon_{U0v'}/kT}. \tag{12}$$

The resulting spectrum, shown in Fig. 6(a), is exceedingly dominated by the sharp peak due to the low v' states. In

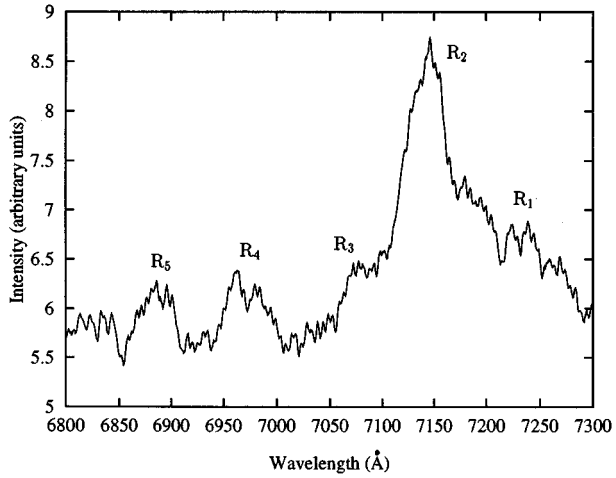

FIG. 5. Emission spectrum of NaCd* in the red region, collected during cw excitation of the Na+Cd mixture, at $T=850$ K and $p=80$ mbar.

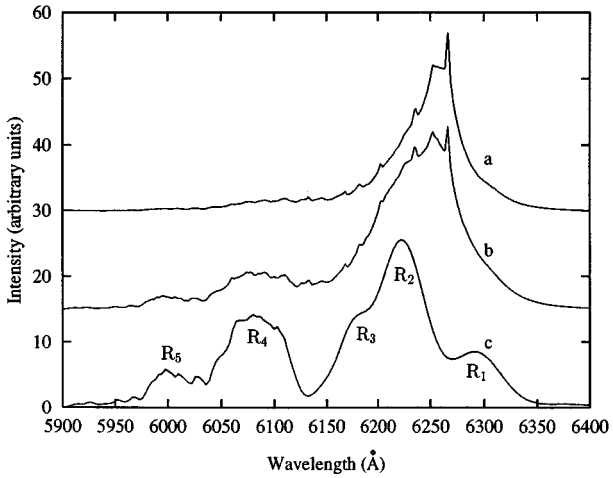

FIG. 6. Emission from the 2 $^2\Sigma^+$ state; a, simulated spectrum, assuming a Boltzmann distribution of the vibrational populations; b, simulated spectrum, assuming a distribution independent of the vibrational energy; c, as before, but limited to $v' \geqslant 8$. The a and b curves are shifted upwards for the sake of clarity.

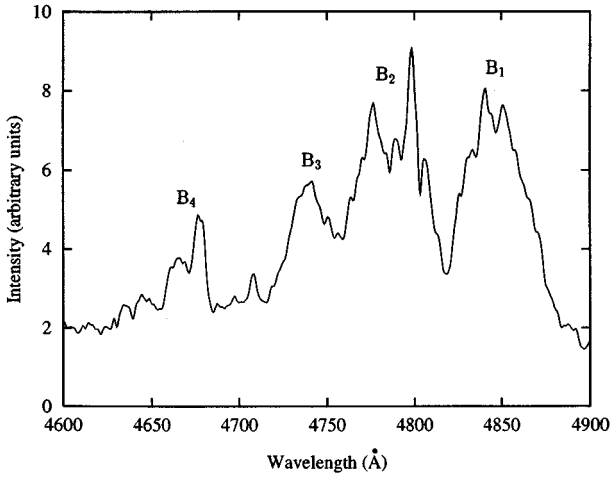

FIG. 7. Emission spectrum of NaCd* in the blue region (resonant pulsed excitation of Cd, $T=720$ K, $p=35$ mbar).

Figs. 6(b) and 6(c) we show the spectra obtained, respectively, with a distribution independent of the vibrational energy:

$$N_{v'} = \text{const} \tag{13}$$

and one limited to the highest states:

$$N_{v'}=0 \quad \text{for } v' \leqslant 7, \qquad N_{v'}=\text{const} \quad \text{for } v' \geqslant 8. \tag{14}$$

Notice that the statistical weight of different vibrational states according to the distributions (13) and (14) is not equal, because a lower v' implies a larger range of allowed J, whose contributions are summed up according to Eq. (8).

In Fig. 6(c) we have shoulders accompanying the main peak, and secondary maxima, as in the experimental spectrum; also the spacing of these oscillations is rather well reproduced, although the whole spectrum should be displaced by about 2000 cm^{-1} (see Table III). The conclusion is that, in the experimental conditions of this work, we are far from a complete thermalization of the vibrational energy of NaCd*. By preferentially populating the lowest vibrational states, one or a few very narrow peaks should appear; when the higher states predominate, several smoother oscillations, with much larger spacings, are produced. The latter behavior is observed by Fijan *et al.*,[2] even more selectively than in our case: they find four maxima with about the same intensities, at 726.5, 709, 697, and 691 nm, while the peak at 714 nm is completely missing. The comparison of the two spectra leads us to conclude that in the experimental conditions of Ref. 2 the vibrational state distribution is shifted towards higher v' than in our case: this can be due, for instance, to the lower buffer gas pressure adopted by Fijan *et al.*

TABLE III. Experimental and computed spacings between maxima in the emission spectra (cm^{-1}).

	Red bands	
	Expt.	Calc.
R_1-R_2	160–180	180
R_2-R_3	130–150	110
R_3-R_4	200–240	265
R_4-R_5	170–190	225
	Blue bands	
	Expt.	Calc.
B_1-B_2	220–230	195
B_2-B_3	220–250	170
B_3-B_4	240–310	230

The blue portion of the emission spectra of NaCd*, produced either with process (1) or with process (2), shows at least three bands,[3,13,16] centered at 473.5, 479.1, and 484.3 nm. In some cases a fourth band at 467 nm is well resolved, as in the spectrum obtained by Cd resonant excitation,[3,16] of which we reproduce the relevant portion in Fig. 7.

The emission from single vibrational states belonging to the 2 $^2\Pi$ potential (blue bands) qualitatively exhibits the same features already seen for the 2 $^2\Sigma^+$ state: a narrow peak for $v'=0$ and smoother oscillations for higher v'. Both the 2 $^2\Pi_{1/2}$ and the 2 $^2\Pi_{3/2}$ may contribute to the blue emission, thus explaining the presence of at least two peaks, separated by about 200 cm^{-1} (50 Å in the wavelength scale). However, the presence of the other peaks must be due to oscillations of the Franck–Condon factors, as in the case of the red bands. Again, this requires a substantial contribution from vibrational states with high v'. In Fig. 8 we show the simulated spectra, considering, in the first instance, the contribution of the 2 $^2\Pi_{1/2}$ state only. If we assume a Boltzmann distribution on the vibrational levels, as in Eq. (13), the queue extending towards shorter wavelengths is not sufficiently structured [see Fig. 8(a)]. A distribution independent of the vibrational energy, Eq. (13), gives rise to a distinctly forked main peak, with a few more maxima [Fig. 8(b)]. Summing up the contributions of both components of the 2 $^2\Pi$ state, we obtain the spectrum of Fig. 8(c), with two forked peaks (B_1 and B_2), another one of similar intensity (B_3),

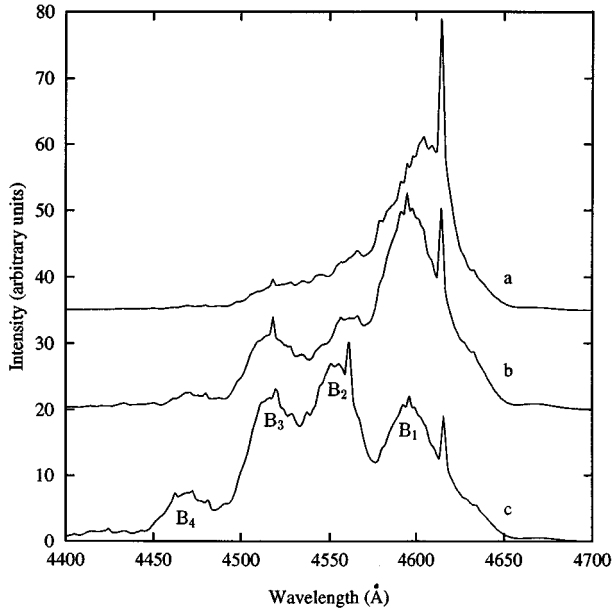

FIG. 8. Emission from the 2 $^2\Pi$ state; a, simulated spectrum, assuming a Boltzmann distribution of the vibrational populations, $^2\Pi_{1/2}$ component only; b, simulated spectrum, assuming a distribution independent of the vibrational energy, $^2\Pi_{1/2}$ component only; c, vibrational distribution as in b, both $^2\Pi_{1/2}$ and $^2\Pi_{3/2}$ components. The a and b curves are shifted upwards for the sake of clarity.

and a lower maximum (B_4), as found experimentally. The central peak B_2 overlaps the queue of B_1, therefore it is more intense. The absolute error in the emission frequencies is about 1000 cm^{-1}, in eccess. The separation between the two main peaks, B_1 and B_2, due to the spin–orbit coupling, is 195 cm^{-1}; experimentally, 220–230 cm^{-1}. Under this respect, NaCd is intermediate between NaZn (no detected spin–orbit splitting)[12] and NaHg. In the latter case, the 3 $^2\Sigma^+$ and 2 $^2\Pi$ states are strongly mixed by spin–orbit coupling, and the three resulting potential curves are separated by 800 and 300 cm^{-1} around their minima; at least two of these states contribute to the emission.[13]

V. CONCLUSIONS

The determination of potential energy curves and the spectral simulations lead us to unequivocally assign the red and blue emission band systems to the 2 $^2\Sigma^+$ and 2 $^2\Pi$ states of NaCd*. The observation of an extended band structure in both cases implies that the excited vibrational states are more populated than allowed by Boltzmann's law: i.e., the excimers are not thermally equilibrated in the experimental conditions. The two main peaks in the blue bands, at 479.1 and 484.3 nm, are assigned to the 2 $^2\Pi_{3/2}$ and 2 $^2\Pi_{1/2}$ components, respectively. The sharp spikes which can be seen in the blue spectrum might dominate both the red and the blue emissions, if a complete thermalization of the excimer would take place, in different experimental conditions.

ACKNOWLEDGMENTS

We wish to express our gratitude to F. A. Gianturco and to S. Milošević for very useful discussions. This work was partially supported by the EEC Network ''Lasers, atoms, and molecules: dynamical interactions'' and by the Austria–Italy Scientific-Technical Agreement.

[1] G. Pichler, D. Veža, and D. Fijan, Opt. Commun. **67**, 45 (1988).
[2] D. Fijan, D. Veža, and G. Pichler, Chem. Phys. Lett. **154**, 126 (1989).
[3] G. De Filippo, Tesi di Laurea, Department of Physics, University of Pisa (1994).
[4] J. P. Woerdman, J. Schlejen, J. Korving, M. C. van Hemert, J. J. de Groot, and R. P. M. van Hal, J. Phys. B **18**, 4205 (1985).
[5] J. Schlejen, J. P. Woerdman, and G. Pichler, J. Mol. Spectrosc. **128**, 1 (1988).
[6] L. Windholz, G. Zerza, G. Pichler, and B. Hess, Z. Phys. D **18**, 373 (1991).
[7] G. Pichler, D. Fijan, D. Veža, J. Rukavina, and J. Schlejen, Chem. Phys. Lett. **147**, 497 (1988).
[8] S. Milošević, X. Li, D. Azinović, G. Pichler, M. C. van Hemert, A. Stehouwer, and R. Düren, J. Chem. Phys. **96**, 7364 (1992).
[9] X. Li, S. Milošević, D. Azinović, G. Pichler, R. Düren, and M. C. van Hemert, Z. Phys. D **30**, 39 (1994).
[10] M. C. van Hemert, D. Azinović, X. Li, S. Milošević, G. Pichler, and R. Düren, Chem. Phys. Lett. **200**, 97 (1992).
[11] D. Gruber, M. Musso, L. Windholz, M. Gleichmann, B. A. Hess, F. Fuso, and M. Allegrini, J. Chem. Phys. **101**, 929 (1994).
[12] D. Azinović, X. Li, S. Milošević, G. Pichler, M. C. van Hemert, and R. Düren, J. Chem. Phys. **98**, 4672 (1993).
[13] L. Windholz, M. Musso, G. Pichler, and B. A. Hess, J. Chem. Phys. **94**, 3366 (1991).
[14] M. Musso, L. Windholz, F. Fuso, and M. Allegrini, J. Chem. Phys. **97**, 7017 (1992).
[15] D. Gruber, U. Domiaty, L. Windholz, H. Jäger, M. Musso, M. Allegrini, F. Fuso, and A. Winkler, J. Chem. Phys. **100**, 8103 (1994).
[16] M. Allegrini, G. De Filippo, F. Fuso, D. Gruber, L. Windholz, and M. Musso, Chem. Phys. **187**, 73 (1994).
[17] D. Azinović, S. Milošević, and G.Pichler, Chem. Phys. Lett. **233**, 477 (1995).
[18] S. Milošević, in *Spectral Line Shapes* (in press).
[19] E. Czuchaj, F. Rebentrost, H. Stoll, and H. Preuss, Chem. Phys. **199**, 47 (1992).
[20] C. Angeli, Tesi di Laurea, Department of Chemistry and Ind. Chem., University of Pisa (1994).
[21] C. Angeli and M. Persico (to be published).
[22] P. J. Hay and W. R. Wadt, J. Chem. Phys. **82**, 270 (1985).
[23] R. Cimiraglia, J. Chem. Phys. **83**, 1746 (1985).
[24] R. Cimiraglia and M. Persico, J. Comput. Chem. **8**, 39 (1987).
[25] M. Persico, in *Spectral Line Shapes*, edited by F. Rostas (De Gruyter, Berlin, 1985), Vol. 3, pp. 587–613.
[26] R. Cimiraglia, J.-P. Malrieu, M. Persico, and F. Spiegelmann, J. Phys. B **18**, 3073 (1985).
[27] C. E. Moore, *Atomic Energy Levels* (National Bureau of Standards, Washington, DC, 1949).
[28] R. S. Mulliken, J. Chem. Phys. **55**, 309 (1971).
[29] F. Y. Hajj, J. Phys. B **13**, 4521 (1980).
[30] U. Fano, Phys. Rev. **124**, 1866 (1961).
[31] R. Cimiraglia, M. Persico, and J. Tomasi, Chem. Phys. **42**, 297 (1979).